Development of a Three-Element Beam Steering Antenna for Bearing Determination Onboard a UAV Capable of GNSS RFI Localization

Adrien Perkins, *Stanford University*
Yu-Hsuan Chen, *Stanford University*
Wei Lee, *Edwards Air Force Base*
Sherman Lo, *Stanford University*
Per Enge, *Stanford University*

BIOGRAPHIES

Adrien Perkins is a Ph.D. candidate in the GPS Research Laboratory at Stanford University working under the guidance of Professor Per Enge in the Department of Aeronautics and Astronautics. He received his Bachelor of Science in Mechanical Aerospace Engineering from Rutgers University in 2013 and his Master of Science in Aeronautics and Astronautics from Stanford University in 2015.

Yu-Hsuan Chen is a research engineer at the Stanford University GPS Laboratory.

Wei Lee is an Electronic Warfare Engineer at the 412th Electronic Warfare Group, Edwards Air Force Base, CA. He was recently selected for a rotational assignment to the 412th Test Wing Test Safety Office where he is responsible for conducting independent safety review on all projects executing at Edwards AFB. His previous experience includes electronic warfare and weapons testing on F-16, F-22, F-35, B-1, and B-2 platforms. He received his Bachelor of Science in Aerospace Engineering from the University of California Los Angeles and his Masters of Science in Aeronautics and Astronautics from Stanford University.

Sherman Lo is a senior research engineer at the Stanford University GPS Laboratory.

Per Enge is a Professor of Aeronautics and Astronautics at Stanford University, where he is the Vance and Arlene Coffman Professor in the School of Engineering. Here, he directs the GPS Research Laboratory which develops navigation systems based on the Global Positioning System (GPS).

ABSTRACT

Localization of radio frequency interference (RFI) sources requires some method of measuring the interference signal. A technique used for this problem in the past, coupled with an unmanned aerial vehicle (UAV), is using a collection of signal strength measurements to determine bearing to the source. This paper focuses on the improvements from a physical rotation based system to an electronic rotation system. Previously 30 seconds was required to collect a set of signal strengths to use for a bearing and now, with a beam steering antenna, that rotation time is reduced to just over 0.5 seconds.

Here, the improvements to the measurement sensor onboard a UAV for RFI localization are detailed. Using the same philosophy to get bearing from a collection of signal strength measurements, these improvements move from a physical rotation to an electronic rotation through the development of a small and compact three-element beam steering antenna. Using this type of antenna allows for signal strength measurements at 500Hz and in motion and therefore enables a much higher observation rate, on the order of 2Hz, enabling the use of different navigation and path planning algorithms that could lead to much faster and more efficient localization. This paper describes the design, development and testing of the beam steering antenna itself, the algorithms for controlling the beam steering to be able to get the best observation performance, and finally demonstrates the performance of the antenna during live interference exercises at Edwards Airforce Base (AFB).

INTRODUCTION

When it comes to GNSS radio frequency interference (RFI) localization, a reliable observation of the signal source is always needed, whether it be some way to determine range to the source, bearing to the source, or by other means. Given that one of the simplest and reliable measurements to make of a signal source is signal strength, many methods are built using those measurements as a core for creating a more useful observation. For example, some methods simply use signal strength as an indicator for a range measurement, however this technique is notoriously unreliable [1]. Another technique, used in this paper, is the ability to use a collection of signal strength measurements to accurately determine the bearing to the source. A system based on this technique has been previously used on an autonomous multirotor unmanned aerial vehicle (UAV) capable of localizing GNSS interference [2].

Previous System

In previous work, a directional antenna was mounted onboard a multirotor UAV platform to make signal strength measurements. The collection of measurements at different azimuths was achieved through the physical rotation of the vehicle (and therefore the antenna) which took approximately 30 seconds to complete [2]. Due to the very low rate of observations, and the physical rotation required to make the observation, an algorithm was designed to determine the best locations for observations to be made from to localize the jammer as quickly as possible. This brings to light two of the major limitations of this systems: the time required to make an observation and the need for accurate navigation to make observations at specific near optimal locations. Furthermore, due to the low rate of observations, this method would only work on a single fixed interference source.

The goal of this work is to improve the measurement method to greatly increase the observation rate. By developing a beam steering antenna and electronically rotating the antenna beam, the observation rate can be increased significantly. This will also enable new localization algorithms and navigation techniques to overcome the previous limitations of need a fixed interference source and accurate navigation. Two key benefits of a high rate of observation is the ability to localize and track moving sources and the ability to incorporate simultaneous localization and mapping (SLAM) techniques to both localize the interference source and navigate successfully without GPS by using that same source as a beacon, or signal of opportunity.

To achieve these benefits, a compact and steerable three-element beam steering antenna was developed to electronically steer the antenna beam at a much higher rate. Careful consideration needed to be made in the design and construction of the antenna to ensure proper performance, namely accurate steering and high sensitivity with robustness to noisey environments.

DEVELOPMENT

To design a beam steering antenna to work well onboard a UAV, the antenna should to be compact, lightweight and reliable. To that end, a three-element array using phase shifters for steering both the azimuth and elevation of the beam was designed and developed. To optimally steer the beam, each element of the antenna array was designed carefully to have equal electrical phase delay before the phase shifters. A calibration was needed to measure the true phase delay which is then compensated with the phase shifters.

Another key element of this antenna system is that instead of feeding into a typical receiver, the signal feeds into an RF power detector to be able to measure signal strength. The benefit of the RF power detector is that it has a large dynamic sensing range of 70dB [3]. Combined with the steerability, these signal strength measurements allow for the recreation of the gain pattern and therefore determining the bearing to the signal source.

Antenna Design

The antenna elements are laid out on a triangular lattice pattern on a half wavelength rectangular grid (depicted in Figure 1). While a larger spacing would result in a narrower beam, grating lobes would be present which would make it more difficult for bearing extraction [4]. This configuration can also be seen in Figure 2 which shows the completed antenna board.

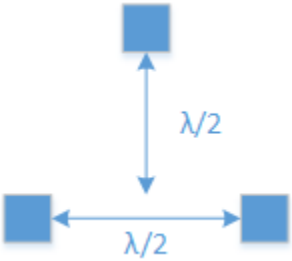

Figure 1: antenna element layout with a spacing of a half wavelength

There are two common choices for GPS L1 antennas: helical and patch antennas, such as the ones shown in Figure 3. Using a helical antenna for each element results in a narrower beamwidth (60 degrees) than using a patch antenna as the element (100 degrees), as shown in the theoretical gain patterns for these two antenna types in Figure 4. However, patch antennas on the market tend to have higher efficiencies and therefore are capable of picking up weaker signals, which proved to be a key element for our flight testing. To test the performance of several different antennas, the board is designed with SMA connectors (shown in Figure 2) to connect the antennas, providing the ability to run tests with multiple different types of antennas.

(a) (b)

Figure 3: example (a) helical and (b) patch antennas used as antenna elements

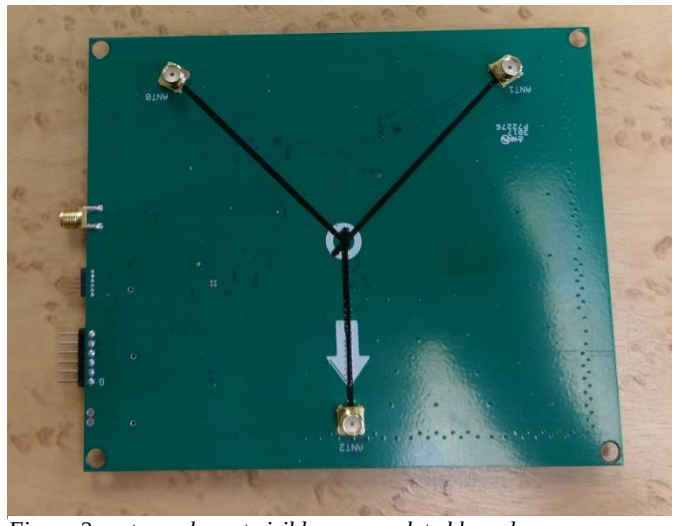

Figure 2: antenna layout visible on completed board

While these two types of antennas have very different beamwidths, they both suffer from large side lobes when steered, as shown in a theoretical steered pattern depicted in Figure 5. These side lobes are due to the combination of the three different elements into a single beam. The size of the side lobes present are primarily a function of the desired elevation angle, with small side lobes present for small desired elevation angles and grow to be nearly the same size as the main lobe when trying to steer to the horizon. Previous bearing calculation methods were designed with only one main lobe in mind [5], so modifications were required to extract multiple possible bearings. When steering to the horizon this poses a problem of having several possible bearings options, however, using the right type of filter for localization can solve the problem of which bearing is correct, as one will provide a converging localization solution and the other will provide a diverging solution.

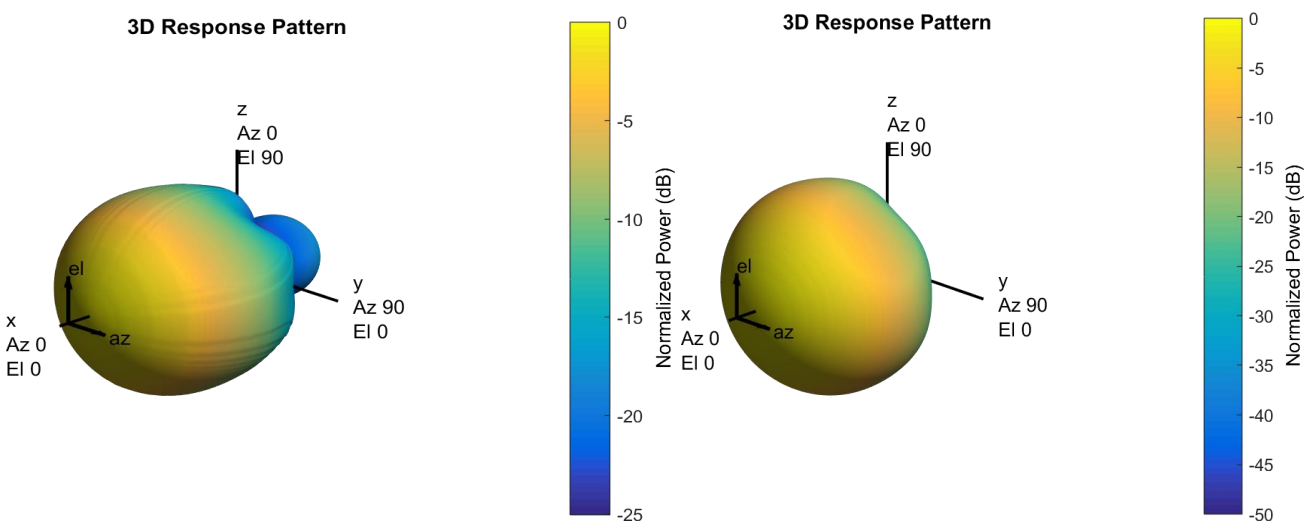

(a) (b)

Figure 4: theoretical antenna gain patterns for (a) helical antenna element and (b) patch antenna element

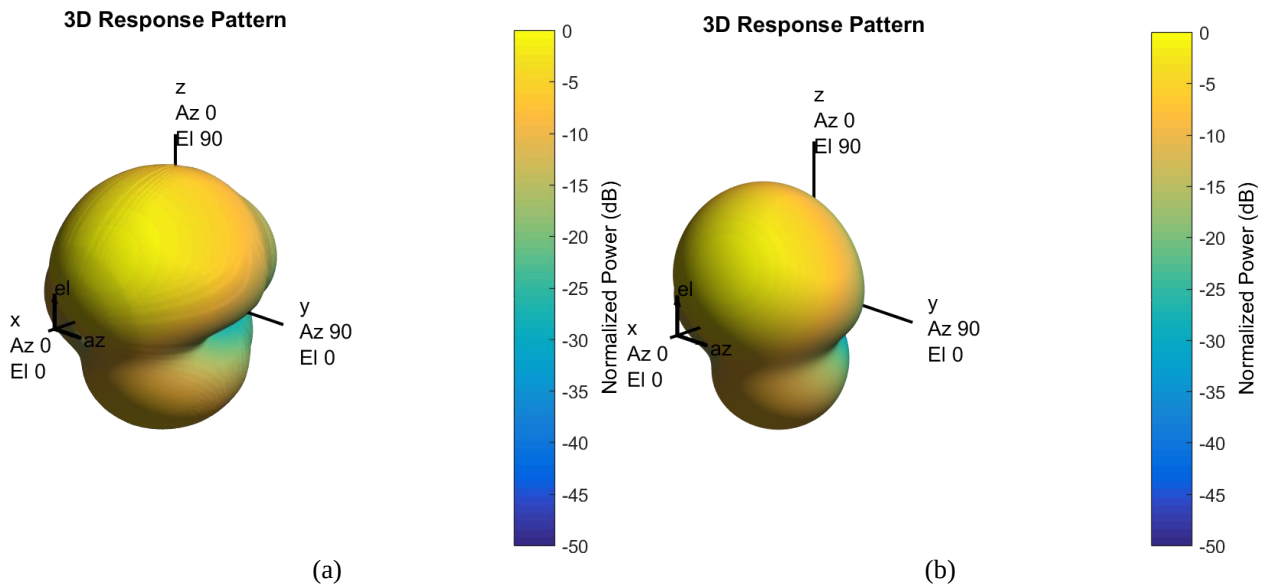

Figure 5: theoretical antenna gain patterns for (a) helical antenna elements and (b) patch antenna elements steered to point at 45 degrees of azimuth and elevation

Antenna Schematic

The overall schematic of the antenna is shown in Figure 7 and Figure 8. As detailed in Figure 8, the signal from each antenna element was passed through three key components before being combined in the power combiners: a SAW filter, an LNA and a phase shifter.

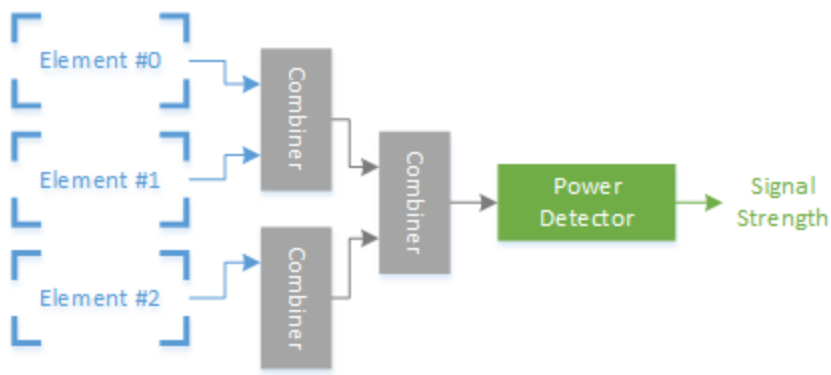

Figure 6: schematic of components for beam steering antenna

The 15MHz wide SAW filter ensures the power levels being measured by the system is only due to interference right around the GPS L1 frequency where an interference device will typically broadcast [5]. The 20dB LNA boosts the power level of the incoming signal to increase the sensitivity, and therefore the operating range, of the antenna. The 8-bit phase shifters provide the necessary control over the phase on the incoming signals to successfully steer the resulting beam in the desired two dimensions. Each of these three feeds are then combined in a set of power combiners before finally going to an RF power detector. The power detector simply measures the signal strength of the incoming signal, proving the core measurement to eventually get a bearing observation.

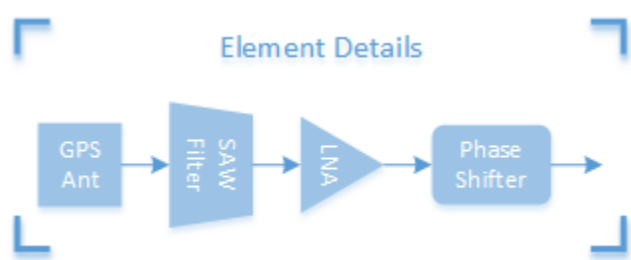

Figure 7: detailed view of components for each antenna element

Calibration

When placing the components on the PCB itself careful consideration needed to be made to ensure the signal from each antenna element was affected similarly. However, even when being very careful with the design of the PCB, biases on the board were be present. While the design minimized possible sources for those biases, the biases still needed to be determined for accurate control of the antenna beam with the phase shifters.

Calibration of the antenna was done in a shielded anechoic chamber with a transmit antenna pointed straight down at the antenna as shown in Figure 9. The transmission antenna was set to broadcast a continuous wave signal at 1575.42MHz and power measurements were made at all 65,025 possible phase shift combinations. This yielded the plot shown in Figure 9a, with yellow being the strongest signal strength and blue being the weakest and the center of the plot marking 0 phase shift for antennas 0 and 1.

With the broadcasting antenna along the boresight of the beam steering antenna, peak measured power should occur at 0 phase offset (the center of the figure). However, when looking at the resulting measurements in Figure 9a, the area of peak power (colored yellow on the plot) is not in the center of the plot due to biases on the board. The calculated biases from several different measurement runs were averaged and used to adjust the test, successfully centering the peak as shown in Figure 9b.

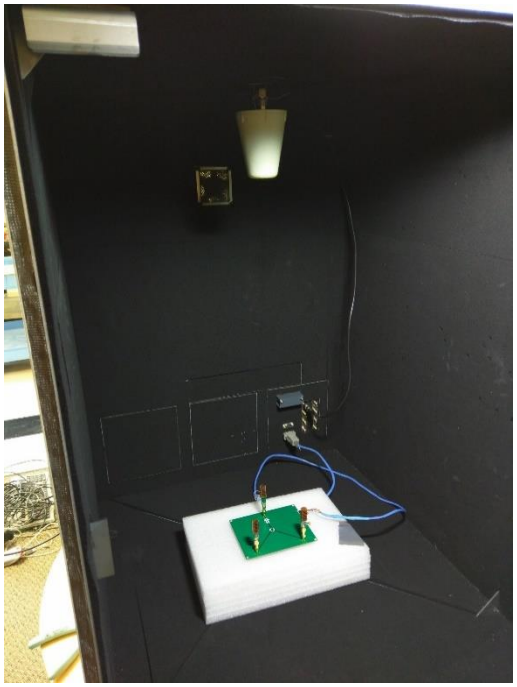

Figure 8: calibration chamber with source antenna (top) and beam steering antenna (bottom)

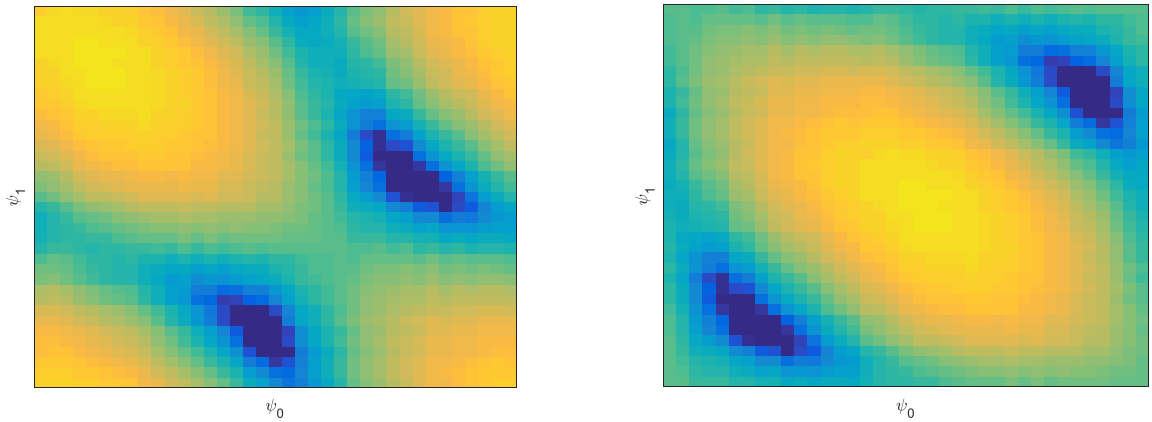

(a) (b)

Figure 9: signal strengths measured for all phase combinations during calibration (a) before and (b) after bias taken into account

Board Operation

To control the beam steering antenna, there is a microcontroller unit (MCU) on the antenna to control each of the phase shifters. The firmware written to control the antenna was designed to operate in two different modes, simply commanding phase shifts, or calculating a desired phase shift from a desired pointing angle and commanding those shifts. To execute the necessary transformations for the control of the phase shifts, several lookup tables were used to ensure the fastest possible performance of the board.

With the RF detector and the MCU, measurements can be made at 500Hz. This means that for a rotation with a measurement at every degree of azimuth, a full rotation is completed in 0.72 seconds, a significant improvement over the nearly 30 seconds for a physical rotation of the vehicle.

Coordinate Systems

There are two coordinate systems of interest that are used with a beam steering antenna: a spherical coordinate system and a phase shifter coordinate system. The spherical coordinate system used has two degrees of freedom, $\phi = [0, 360)$ and $\theta = [0, 90)$, which can also be thought of as the azimuth angle and the angle from the vertical (called elevation in this paper), respectively. Using these two coordinates, the beam can be pointed anywhere in a three-dimensional half sphere. The spherical coordinate system is the natural coordinate system to use to describe the pointing direction of the main beam of the antenna, however, to control the phase shifters to steer the beam a transformation needs to be made.

Having a three-element antenna array provides the two degrees of freedom desired, for example $\psi_1 - \psi_2$ and $\psi_0 - \psi_2$, where ψ_i is the phase set for the ith antenna. Holding one of the antennas to have zero degrees of phase shift (e.g. let $\psi_2 = 0$), simplifies the degrees of freedom to the phase for antennas 0 and 1. With this simplification made, the transformation from the spherical coordinates to the phase shifts can be simplified to the following set of equations [5]:

$$\psi_0 = -\pi * \sin(\theta) * \left(\cos(\phi) + \left(\frac{1}{2}\right) * \sin(\phi)\right)$$
$$\psi_1 = \pi * \sin(\theta) * \left(-\cos(\phi) + \left(\frac{1}{2}\right) * \sin(\phi)\right)$$

From the calibration step explained above, there is one additional element that needs to be taken into account in these equations: the phase bias that may be present on the board for the different antenna elements. Adding b_0 and b_1 as the biases for antenna elements 0 and 1 respectively results in the following set of equations.

$$\psi_0 = -\pi * \sin(\theta) * \left(\cos(\phi) + \left(\frac{1}{2}\right) * \sin(\phi)\right) + b_0$$
$$\psi_1 = \pi * \sin(\theta) * \left(-\cos(\phi) + \left(\frac{1}{2}\right) * \sin(\phi)\right) + b_1$$

To better understand the effects of this non-linear transformation on the pointing angle, consider a constant board level bias of 10 degrees on a single antenna element. The reverse transformation made from the phase shift values to the spherical coordinates results in a non-linear pointing error depicted in Figure 10. This results in matching a measured signal strength with an incorrect pointing angle, distorting the resulting gain pattern and causing errors in bearing observations.

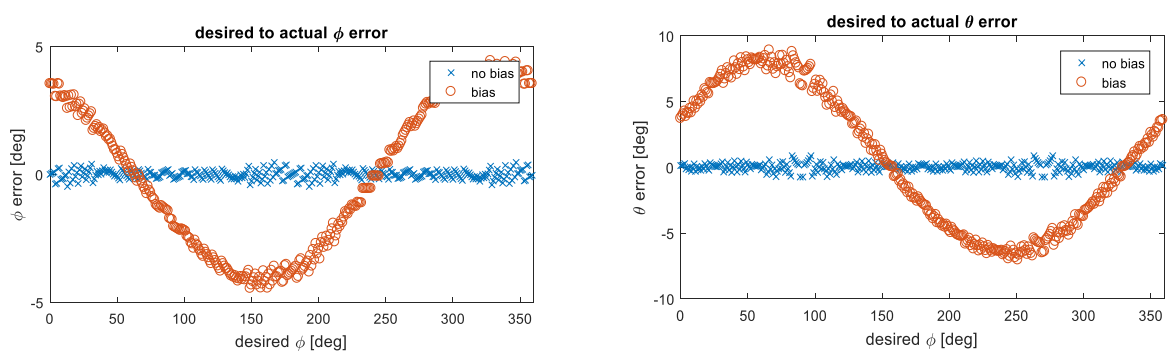

(a) (b)

Figure 10: error in the pointing direction (a) phi (azimuth) and (b) theta (elevation) due to a 10 degree phase bias in antenna 0

This transformation can now be used to convert the plots from Figure 9 to a more understandable frame. Using the inverse of the above transformation equations the signal strengths measured during the calibration tests can be mapped from phase shifts to their respective pointing angles. Cycling through all the different phase shifts results in measurements for a full 360 degrees

of azimuth for nearly each degree of elevation, as shown in Figure 11a. Of more interest may be the result of a single rotation, which can be extracted and is depicted in Figure 11b.

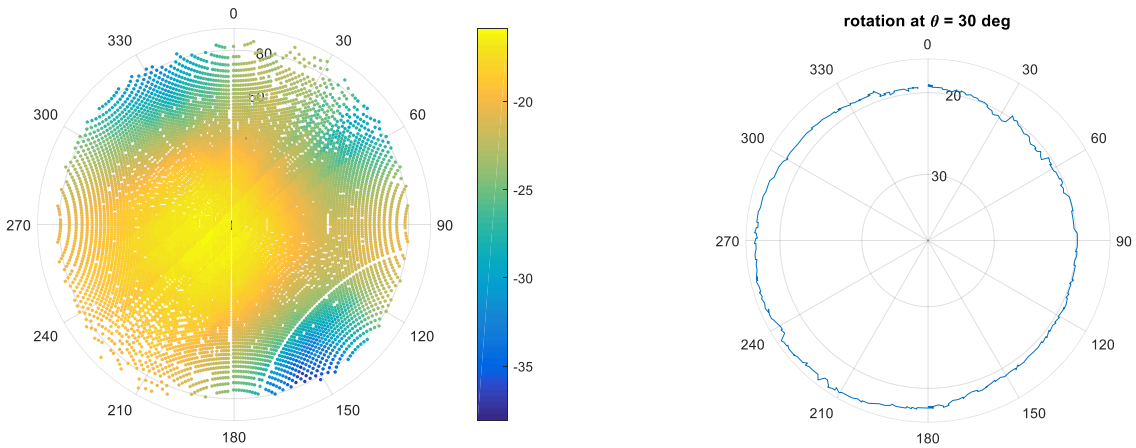

(a) (b)

Figure 11: signal strength measurements in spherical coordinates for (a) all azimuths and elevations and (b) all azimuths at an elevation of 30 degrees

It is worth noting that the patterns in Figure 11 are not perfect as the gain pattern should be a perfect circle (recall the transmission source was placed directly along the boresight of the antenna). This offset is the result of having some slight error in the calibration.

FLIGHT TESTING

To assess the performance of the antenna in a real world environment, the antenna was mounted on a UAV and flown during DT Navfest a live jamming exercise, at Edwards AFB. For the test, the antenna was mounted upside down (main beam pointing straight down) onboard a UAV. During the flights, a GLONASS capable receiver was used for truth position measurements. While the antenna is designed to support multiple antenna types, during the initial flight tests it was determined that the helical antennas were not capable of measuring the interference signal due to their low efficiency, therefore all the test results shown are using a patch antenna.

Tests were done at an altitude of 150m above ground level (AGL) and were focused on ensuring proper performance of the antenna in all directions, therefore measurement sets were made at the same location with rotating the vehicle's heading in steps of 90 degrees.

Figure 12: High power jammer used to create jamming signal

DT Navfest

Flight tests were done during the DT Navfest event on a "non-interference" basis, meaning that we could not dictate any requirements for the tests. This event was the first large scale GPS jamming event held at Edwards AFB (home of the Air Force Test Center) and focused on providing jamming to numerous United States Air Force (USAF) test platforms. To generate the jamming field, six high power jammers (an example of which is shown in Figure 15) and eight smaller portable box jammers were set up around Edwards AFB. Together, these jammers provided an extremely high jammer to signal

ratio (J/S) over Edwards AFB (>85dB at 25k ft). While the jamming was targeted for 25k ft, the jammer's strengths were still plenty strong at 500ft AGL, the altitude of the tests, depicted in Figure 13.

During the three nights of testing, flights were performed at two separate locations, marked on Figure 13. The first location, Location 1, is about 20 km from the collections of jammers in the northwest corner of the map and had J/S levels of about 50 dB. The second location, Location 2, is about 6 km from jammer Hx3 and was subject to J/S levels around 70dB. For another perspective of the jammers from each of the locations, Figure 14 shows the bearing to all of the jammers from each of the two locations colored by distance. These bearings are in world frame and will also be marked on subsequent world frame plots depicting test results.

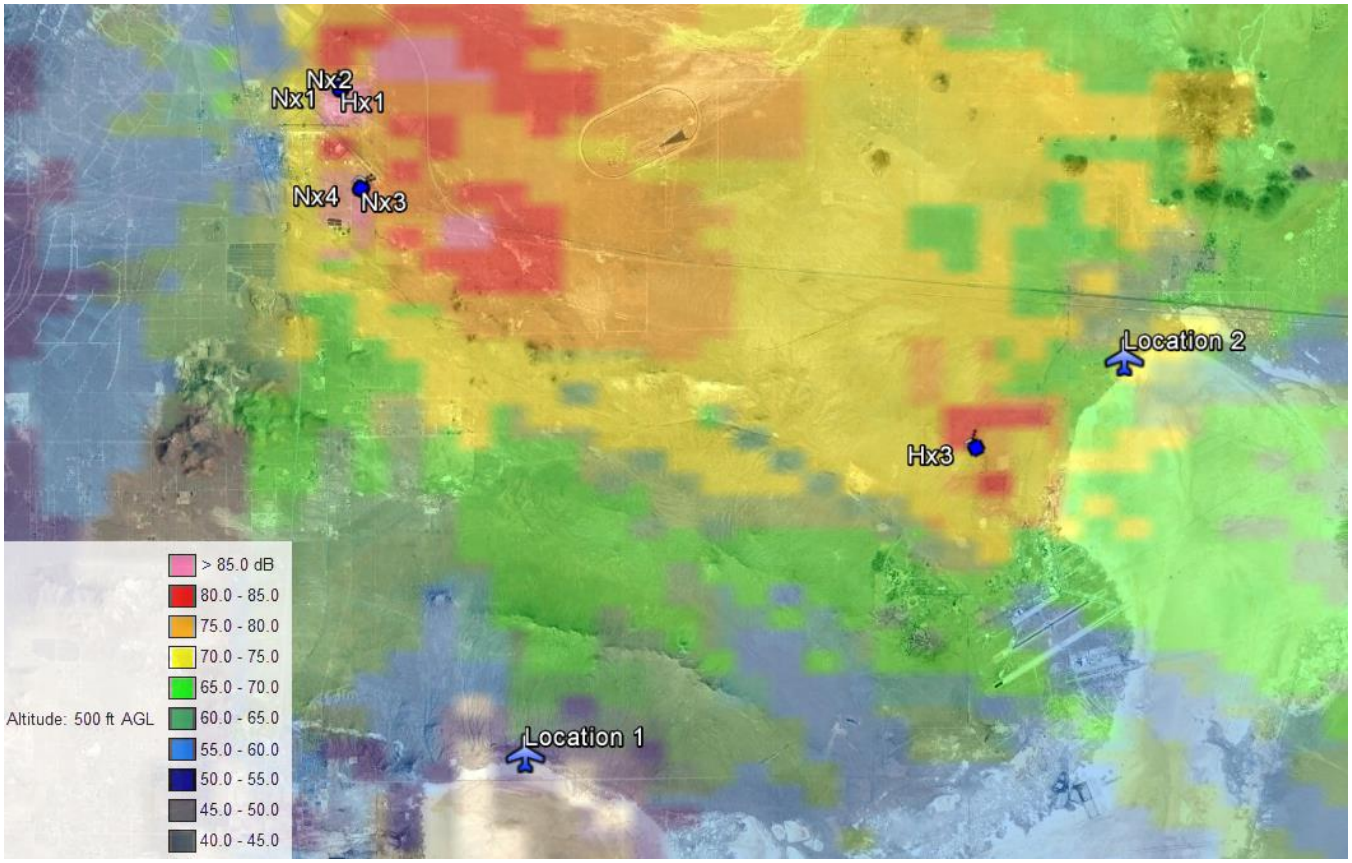

Figure 13: heatmap of jammer to signal ratio at 500ft above ground at Edwards Air Force Base, marked with both flying sites

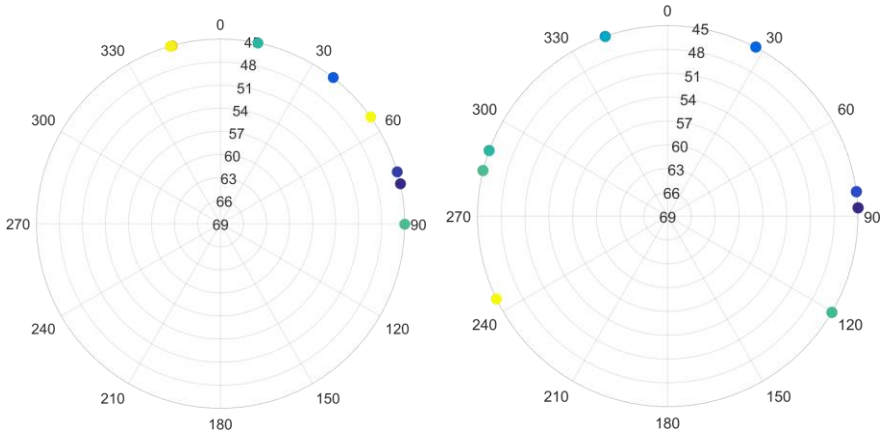

(a) (b)

Figure 14: Bearings to all the jammers from (a) location 1 and (b) location 2 colored by proximity (yellow is closest)

Results

The flight tests aimed at answering three important questions: can the antenna perform in real world noise environment, especially those presented by the UAV's RFI, how sensitive is the antenna, specifically at what power levels can an interference source be detected, and finally, can the bearing be accurately determined from the steered gain pattern, especially with the distortion and secondary lobes that may be present due to the steering which has not previously been encountered.

Looking at Figure 15a, the result of all rotations at elevation angles from 0 to 90 degrees can be seen. Most noticeable is the "peppered" look of the plot compared to the measurements inside the shield chamber caused by noise from both the UAV's operation and just background levels of noise. Extracting just a single rotation, for example one at 60 degrees of elevation as shown in Figure 15b, further depicts the effects of the noise in the pattern. However, using a moving average filter, the noise can be removed and gain pattern (shown as the red line) can be more discernably seen.

One of the next major challenges was determining the bearing from a gain pattern which what appears to be two main lobes. Unable to use previous algorithms due to the presence of two possible lobes, a new method was devised. In this case local maxima were found in the pattern, then the crossing points for 3dB below the power level of the local maxima were found and were averaged to get the bearing of each of the local maxima. In the case of Figure 15b, two local maxima were found, depicted as the green and purple lines perpendicular to the gain pattern. While two different bearings were extracted, for localization, a particle filter can successfully remove the effects of the incorrect (and therefore diverging) bearing observations. These two main lobes are due to the fact that when steering the beam towards the horizon, a fairly large back lobe starts coming in to play. At the distances present in these tests (6km and 20km away), the jammers are effectively on the horizon and therefore a big back lobe becomes present.

Given the effects that a board level bias can have on the effective pointing angle of the beam, and additional two test results are shown for the vehicle being rotated by 90 and 180 degrees, respectively, from the initial position. It is important to note that Figure 15a,c,e are all presented in the body frame of the vehicle (and therefore the area of peak power rotates with the vehicle), while Figure 15b,d,f are in the world frame and therefore, for a perfect antenna, should all be identical.

For a perfect board, Figure 15b,d,f should all point in the same direction. It can be seen that while the gain patterns in Figure 15b and Figure 15f do indeed have a lobe pointed towards the jammer, Figure 15d has a much greater error present in the bearing direction. Looking back at the effects from a board level bias (Figure 10) it can be seen that the maximum and minimum pointing errors are 90 degrees apart, which explains why the middle set of measurements (offset by 90 degrees from the first and last set of measurements) has the worst performance of the set. However, despite these errors, the resulting set of all the bearing measurements at this location only had an error of approximately 4 degrees and a standard deviation of approximately 13 degrees, closely matching the performance of the previous system using a directional antenna [5].

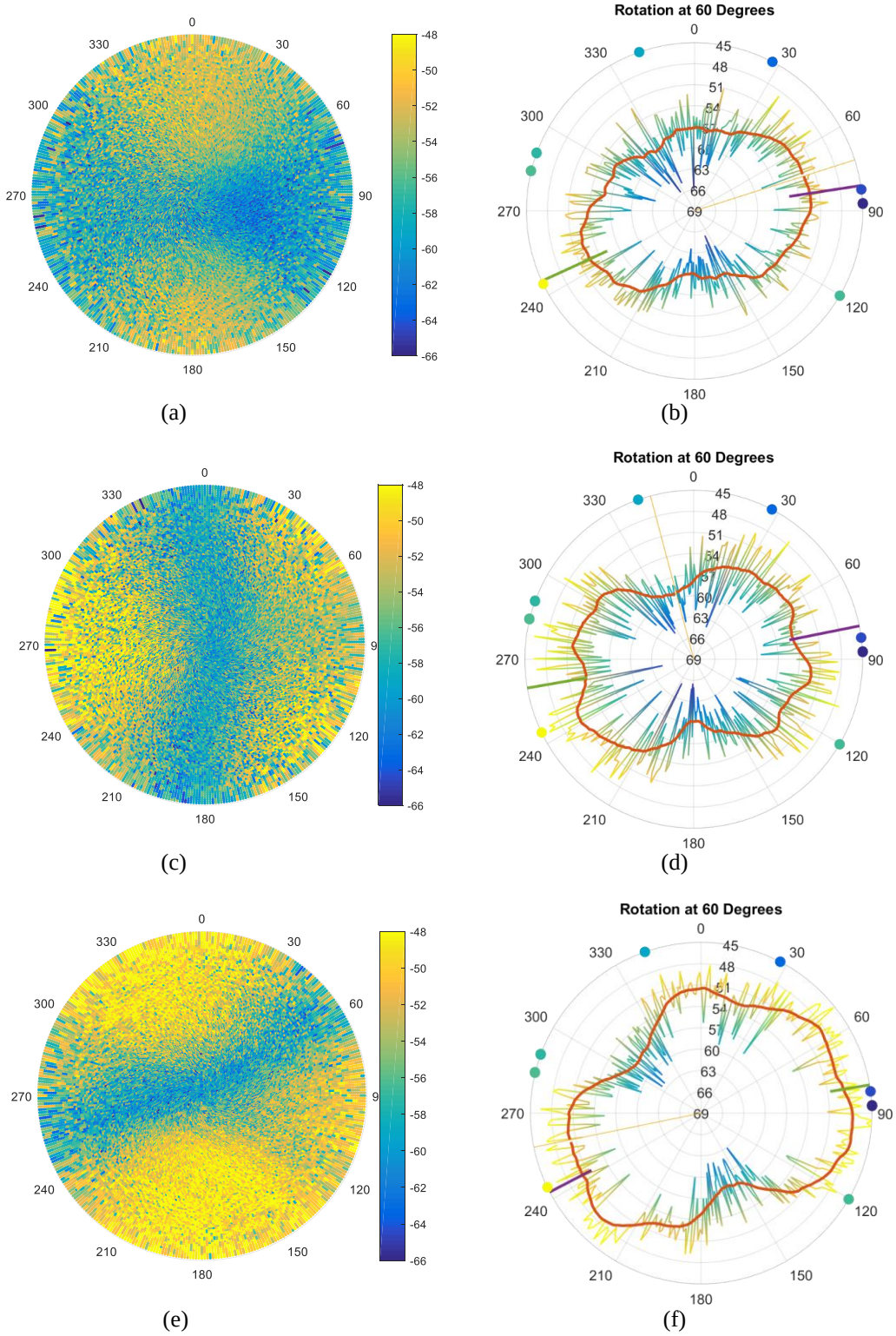

Figure 15: Measured signal strength (a), (c), (e) for all angles and (b), (e), (f) resulting gain patterns at theta = 60 degrees. Measured at a vehicle heading of (a), (b) 90 degrees, (c), (d) 0 degrees, and (e), (f) 270 degrees

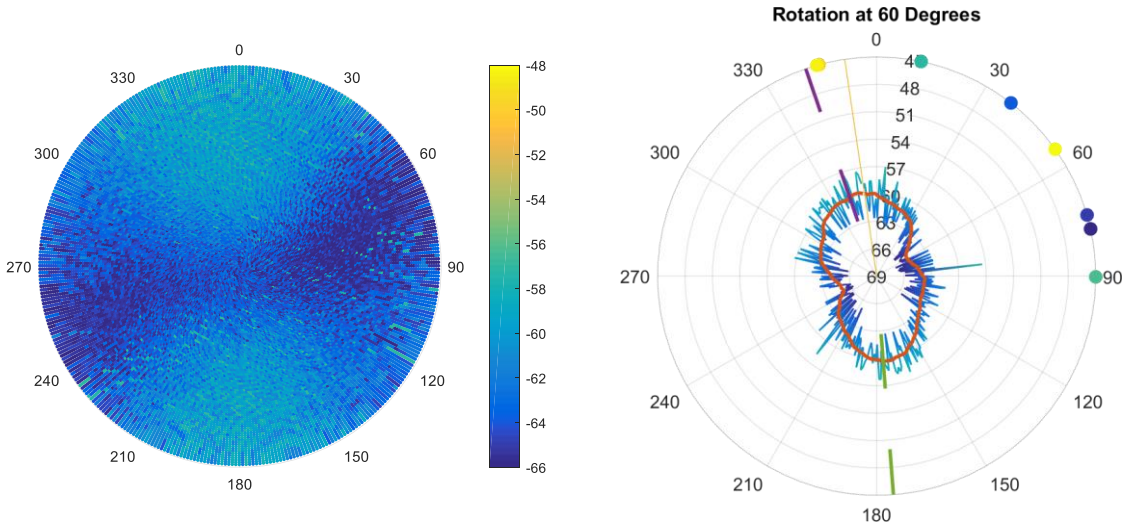

(a) (b)

Figure 16: Measured signal strengths (a) for all angles and (b) resulting pattern at Location 1, a distance of 20km from the jammer

Finally, the tests demonstrated the antenna's sensitivity and ability to still detect and determine a bearing to a jammer at a much lower power level (about 45-50dB) as shown in Figure 16. Note that in this case the body frame plot with all the rotations, Figure 16a, no longer contains any yellow values since the peak powered received was -57dBm, compared to the -45dBm peak power measured in Figure 15, when the jammer was only 6km away and the J/S value was 70dB.

CONCLUSIONS

A compact, steerable three-element beam steering antenna was successfully designed, built, calibrated and tested in a real world jamming environment. The antenna's 500Hz rate of measure enables a bearing observation at a rate of at least 2Hz which is a significant improvement over the 30 seconds rotation periods required when using a directional antenna and physically rotating the UAV. Testing demonstrated the antenna's ability to measure power from a jamming signal as far as 20km away (with a J/S level of 45-50dB). Bearing was able to be determined from the gain pattern measured by the antenna, despite the noisey environment and the large side lobe present due to steering towards the horizon.

The development of this antenna will enable the ability to use new localization algorithms that will be capable of localizing a single moving source in addition to the system's current ability to localize a single fixed jammer. Of even greater interest, the high rate of bearing observations will enable using the jammer's signal as a signal of opportunity for navigation in the GPS denied environment caused by a GPS jammer.

ACKNOWLEDGMENTS

The authors gratefully acknowledge the support of the 412th Test Wing at Edwards AFB and the 746th Test Squadron at Holloman AFB for extending an invitation to test and running the jammers during the DT Navfest event. We thank the Federal Aviation Administration and the Stanford Center for Position Navigation and Time for supporting this research. We also acknowledge Kazuma Gunning for assisting in the flight tests.

DISCLAIMER

The views expressed herein are those of the authors and are not to be construed as official or any other person or organization.

REFERENCES

[1] A. Savvides, C. Han and M. Strivastava, "Dynamic fine grained localization in ad-hoc networks of sensors," in *Proceedings of the 7th annual international conference on mobile networking and computing*, July 2001.

[2] A. Perkins, L. Dressel, S. Lo, T. Reid, K. Gunning and P. Enge, "Demonstration of UAV Based GPS Jammer Localization During a Live Interference Exercise," in *ION GNSS+ 2016*, Portland, OR, 2016.

[3] Linear Technology, "RF Power Detector Datasheet," [Online]. Available: http://cds.linear.com/docs/en/datasheet/5538f.pdf.

[4] A. Perkins, L. Dressel, S. Lo and P. Enge, "Antenna Characterization for UAV Based GPS Jammer Localization," in *ION GNSS+*, Tampa, 2015.

[5] R. H. Mitch, R. C. Dougherty, M. L. Psiaki, S. P. Powell, B. W. O'Hanlon, J. A. Bhatti and T. E. Humphreys, "Signal Characteristics of Civil GPS Jammers," in *ION GNSS*, 2011.

[6] T. C. Cheston and J. Frank, "Phased array radar antennas," in *Radar Handbook*, 1990.